JOURNAL OF NEUROSURGERY:
Case Lessons

J Neurosurg Case Lessons 11(6): CASE25534, 2026
DOI: 10.3171/CASE25534

High-resolution cortical mapping within and across the central sulcus using 1024-electrode micro-electrocorticography arrays: illustrative case

Daniel D. Cummins, MD,[1] Katrina Barth, PhD,[2] Elton Ho, PhD,[2] Alexandra Fink Skular, BS,[3,4] Jacqueline Dister, BS,[2] Benjamin Rapoport, MD, PhD,[1,2] Ignacio Saez, PhD,[1–4] and Joshua B. Bederson, MD[1]

[1]Department of Neurosurgery, Icahn School of Medicine at Mount Sinai, New York; [2]Precision Neuroscience Corporation, New York; [3]Nash Family Department of Neuroscience, Icahn School of Medicine at Mount Sinai, New York; and [4]The Friedman Brain Institute, Icahn School of Medicine at Mount Sinai, New York, New York

BACKGROUND Central sulcus identification using phase reversal on electrocorticography (ECoG) is a critical tool for neurosurgical intervention around the primary motor and somatosensory cortices. This mapping is typically performed using cortical arrays with a resolution of several millimeters.

OBSERVATIONS A 30-year-old female underwent a right frontoparietal craniotomy for resection of a 4-cm contrast-enhancing lesion within the central sulcus. Central sulcus localization was performed using a standard ECoG array. High-resolution micro-ECoG (μECoG) arrays were then placed over the pre- and postcentral gyri, giving 2048-electrode recordings across the central sulcus. Combining this high-resolution μECoG with an augmented reality imaging overlay to identify the tumor, the central sulcus was split, revealing the underlying tumor. A safe, gross-total resection was obtained with no postoperative complications. Through the use of μECoG arrays spanning into the central sulcus, a high-resolution phase-reversal contour was identified across the central sulcus.

LESSONS The authors demonstrate the feasibility and utility of μECoG for sensorimotor mapping within the central sulcus, revealing a phase reversal at a resolution of approximately 400 microns. Compared to standard mapping, which records gyral surface electrophysiology, they further demonstrate phase-reversal electrophysiology within a dissected central sulcus. High-resolution cortical mapping from μECoG may foster several neurosurgical advancements, from tumor resection to brain-computer interfaces.

https://thejns.org/doi/abs/10.3171/CASE25534

KEYWORDS brain tumor; central sulcus; ECoG; mapping; SSEP

A body of work has explored central sulcus morphology using electrocorticography (ECoG).[1,2] One common method to identify the central sulcus is by identification of the phase reversal from somatosensory evoked potentials (SSEPs) from the precentral gyrus to the postcentral gyrus. This mapping is typically performed using cortical strip arrays with a resolution of several millimeters. A complex relationship between the central sulcus and sensorimotor function has been suggested, including an overlap between sensory and motor functions across the central sulcus, and considerable across-subject variability.[1,2] Yet, these findings were limited by traditional low-resolution ECoG arrays. Novel micro-ECoG (μECoG) arrays, with a resolution on the order of microns, have demonstrated significant promise for improved cortical mapping. Thus far, experimental application of μECoG has been largely limited to animal models.[3,4] In this case, we demonstrate the feasibility and utility of μECoG for sensorimotor mapping within the central sulcus using two 1024-electrode arrays.

Illustrative Case

Methods

A 30-year-old female with a history of breast cancer presented with episodic left-hand weakness, numbness, and seizure. A contrast-enhanced brain MRI study demonstrated a 4-cm contrast-enhancing lesion within the right central sulcus (Fig. 1). The patient was neurologically intact on preoperative examination. The patient was taken to the operating room for a right frontoparietal craniotomy for tumor resection. Informed consent was obtained separately for surgical intervention and for research related to use of the high-resolution μECoG array. Local IRB approval was obtained for prospective use of the array and related studies. A nonsignificant risk study was approved by the institutional IRB. Since the patient reported in this case report was enrolled, the brain-contacting component of the research device has received 510(k) clearance from the FDA. Following dural opening

ABBREVIATIONS BCI = brain-computer interface; ECoG = electrocorticography; μECoG = micro-ECoG; SSEP = somatosensory evoked potential.

INCLUDE WHEN CITING Published February 9, 2026; DOI: 10.3171/CASE25534.
SUBMITTED July 12, 2025. **ACCEPTED** December 5, 2025.
© 2026 The authors, CC BY-NC-ND 4.0 (http://creativecommons.org/licenses/by-nc-nd/4.0/)

Unauthenticated | Downloaded 02/21/26 07:00 PM UTC

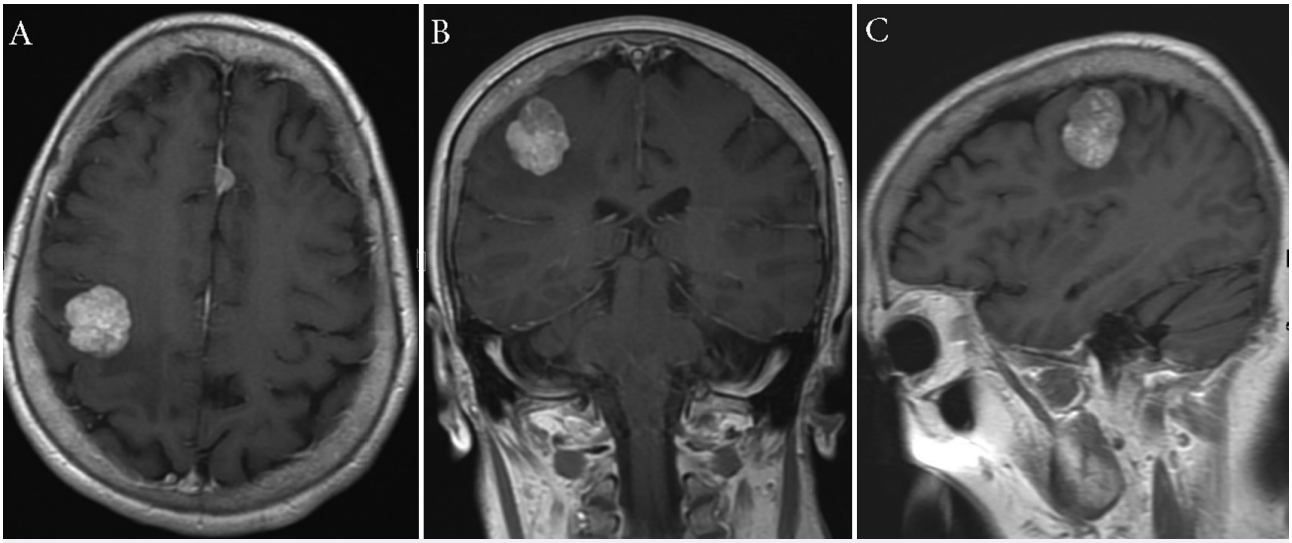

FIG. 1. T1-weighted postcontrast axial (**A**), coronal (**B**), and sagittal (**C**) MR images demonstrating the tumor within the right central sulcus.

and cortical exposure, the right central sulcus was identified using a standard ECoG strip array by median nerve SSEPs. A clear site of phase reversal was seen between electrode 3 (precentral gyrus) and electrode 5 (postcentral gyrus) on the strip array, with electrode 4 (central sulcus) isoelectric. Two separate Precision 1024-electrode μECoG arrays were then placed over the pre- and postcentral gyri, giving 2048-electrode recordings across the central sulcus. Each μECoG array was made of a thin (22 μm) polyimide substrate with 1024 platinum microcontacts (977 contacts of 50 μm in diameter, 42 of 380 μm in diameter, and 5 of 500 μm in diameter). The arrays were bonded to printed circuit boards with Intan RHD2000 amplifier chips (Intan Technologies), which amplified with a bandwidth of 0.1–7.5 kHz and digitized at a sampling rate of 20 kilosample/sec. The recording reference was connected to a needle electrode in the scalp at the Fz position, and ground was connected to a needle electrode in the shoulder. Impedance was recorded once both arrays were placed on the cortical surface, and only recording contacts with impedances < 4 MΩ were included for analysis (90.9% of all channels). The mean and standard deviation of impedance for included channels was 1.09 ± 0.33 MΩ.

Results

Figure 2 demonstrates a comparison between the 1024-electrode Precision array with standard 4–8 electrode ECoG strip arrays used for neurosurgical mapping. Once the Precision μECoG arrays were placed, the standard ECoG array was removed. The central sulcus was then opened, and one μECoG array was positioned from the precentral gyrus onto the anterior central sulcus, while the second μECoG array was positioned from the posterior central sulcus onto the postcentral gyrus.

While standard mapping approaches with ECoG record only the superficial cortical surface of the precentral gyrus and postcentral gyrus (Fig. 3A), this case with central sulcus dissection and flexible μECoG arrays allowed recordings from four different surfaces: 1) precentral gyrus cortical surface, 2) anterior central sulcus, 3) posterior central sulcus, and 4) postcentral gyrus cortical surface (Fig. 3B). Figure 4 demonstrates standard ECoG and μECoG recordings prior to central sulcus dissection. A clear phase reversal at approximately 20 msec from median nerve stimulation is seen between ECoG contact 5 (Fig. 4C, postcentral gyrus) and ECoG contact 3 (Fig. 4F, precentral gyrus). Micro-ECoG contacts corresponding to the same regions of cortex matched the same waveform morphology as seen with standard ECoG. Figure 4I demonstrates the spatial and temporal evolution of μECoG SSEPs across the central sulcus. With a boundary of the central sulcus defined by standard ECoG recordings (dotted line), a high-resolution SSEP phase-reversal boundary is reflected by the dynamic heatmap from 16 to 30 msec following median nerve stimulation. Figure 5 demonstrates μECoG activity after central sulcus dissection, with each μECoG array folded into the central sulcus to enable recordings within the central sulcus. With each array spanning the dissected central sulcus, again a spatiotemporal evolution of the phase reversal from 16 to 30 msec after median nerve stimulation is seen.

Tumor resection was aided by use of an intraoperative augmented reality imaging overlay (heads-up display, previously described).[5] Use of the heads-up display and high-resolution μECoG mapping to enter the central sulcus for resection enabled a safe, gross-total resection with no immediate postoperative complications. At long-term follow-up after 6 months, the patient remained at neurological baseline with no tumor recurrence. Video 1 includes a comprehensive presentation of this case.

VIDEO 1. Video demonstration of the operative case and use of Precision μECoG arrays for mapping within the central sulcus. Click here to view.

Informed Consent

The necessary informed consent was obtained in this study.

Discussion

Observations

The primary motor cortex and primary somatosensory cortex are two of the most critical functional regions of the brain. Preservation of these regions using cortical mapping is essential in neurosurgical

Unauthenticated | Downloaded 02/21/26 07:00 PM UTC

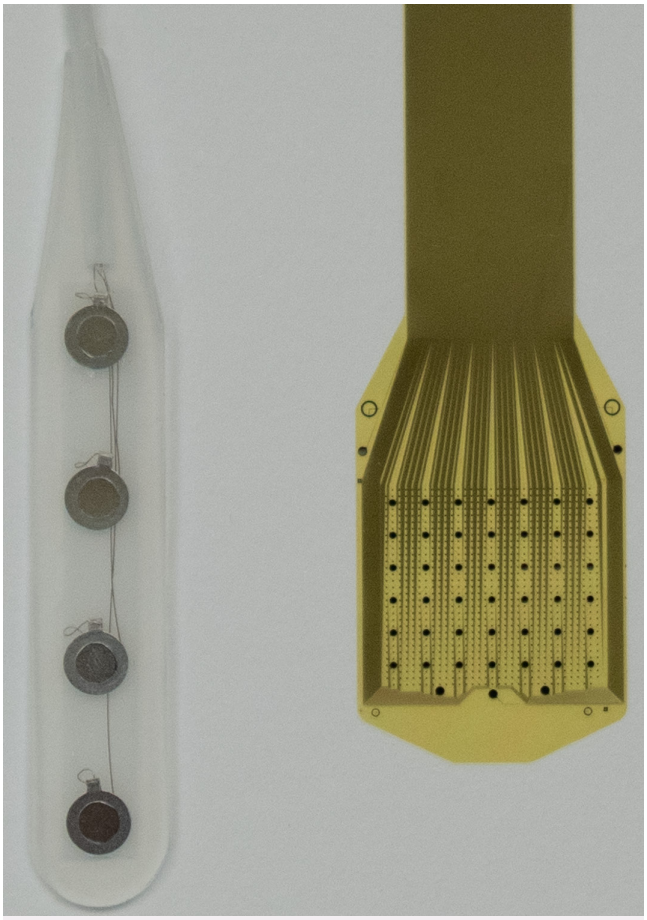

FIG. 2. The Precision Layer 7 µECoG array (*right*) contains 1024 electrodes ranging in diameter from 50 to 380 µm. In contrast, standard ECoG arrays (*left*) contain 4–8 electrodes with spacing of several millimeters. The Precision array covers a surface area of approximately 1.5 cm^2. The 1024 surface microelectrodes include 977 electrodes at 50 µm in diameter, 42 electrodes at 380 µm, and 5 electrodes at 500 µm. Each electrode is spaced 400 µm apart.

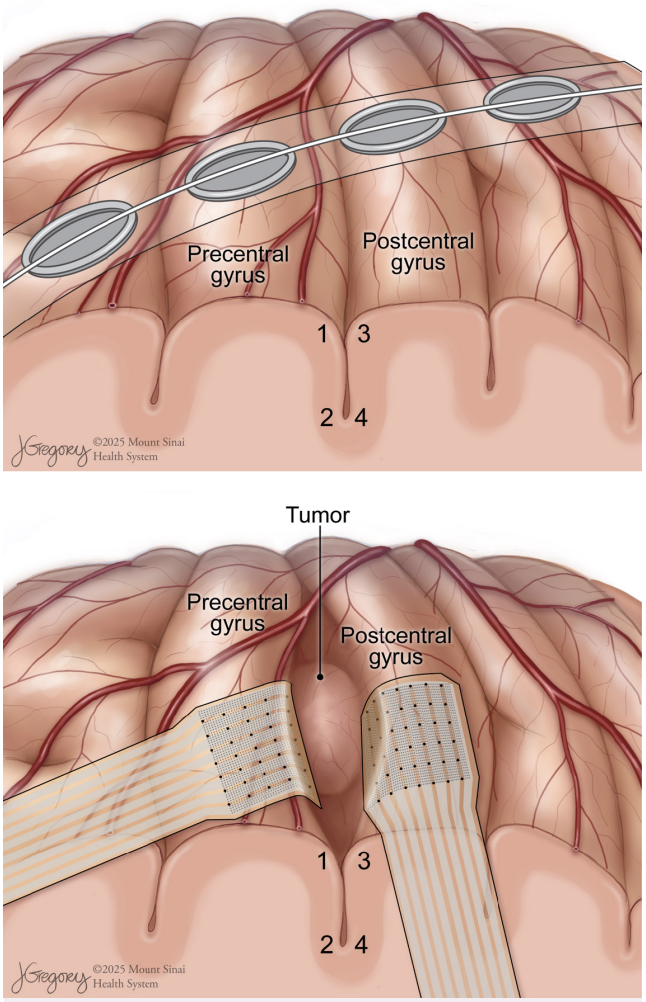

FIG. 3. Standard phase-reversal mapping versus µECoG mapping into the central sulcus. **Upper Panel:** The standard SSEP strip array captures only the cortical surface of the precentral and postcentral gyri. With use of this technique, the surfaces of the central sulcus are not in contact with the electrode array, leaving the function and electrophysiology of the cortex within the central sulcus itself uncaptured. **Lower Panel:** The presented case differed from standard mapping in two ways: 1) use of a flexible Precision 1024-electrode µECoG array, and 2) dissection of the central sulcus, which allowed the electrode arrays to be placed on the sulcal cortex. These two factors enabled high-resolution recordings spanning the precentral gyrus (1), anterior (2) and posterior (3) surface of the central sulcus, and postcentral gyrus (4).

intervention, such as in this case of tumor resection around the central sulcus. We demonstrate a high-resolution phase reversal spanning into the central sulcus, which varies in both space and time. Using traditional millimeter-resolution ECoG grids for mapping, we can see patient-specific unique morphologies of reversal in polarity between the precentral and postcentral gyri.[6,7] Our demonstration of high-resolution phase-reversal mapping reflects two unique elements of this case: 1) implementation of flexible µECoG arrays, yielding 2048 total electrodes over the precentral and postcentral gyri with 400-micron resolution, and 2) placement of electrodes spanning the deeper portions of the central sulcus. While standard strip electrode monitoring of phase reversal provides only an isoelectric point, the high-resolution grid phase reversal demonstrated in this case provides a phase-reversal "contour line," which can also demonstrate high-resolution temporal changes. Wang et al. demonstrated a case of µECoG recordings over the precentral gyrus in a human patient (all electrodes placed anterior to the central sulcus). This case appeared to demonstrate a reversal in polarity over the precentral gyrus with individual finger movement.[8] However, this case was limited by a µECoG array consisting of 16 electrodes, and by recordings only over the precentral gyrus, rather than both the precentral and postcentral gyri.[8] Kaiju et al. demonstrated in nonhuman primate experiments that there are clear differences in the morphology of SSEPs between 128-channel and 1152-channel μECoG arrays. In particular, their work revealed high-resolution complex contours of phase reversal using 1152-channel arrays that were not revealed with 128-channel arrays.[3]

In addition to use of a 1024-electrode µECoG array, this case is also distinguished by placement of electrodes within the central sulcus, as opposed to standard SSEP mapping, usually limited to the surface of the precentral and postcentral gyri (Fig. 3). Other work in

Unauthenticated | Downloaded 02/21/26 07:00 PM UTC

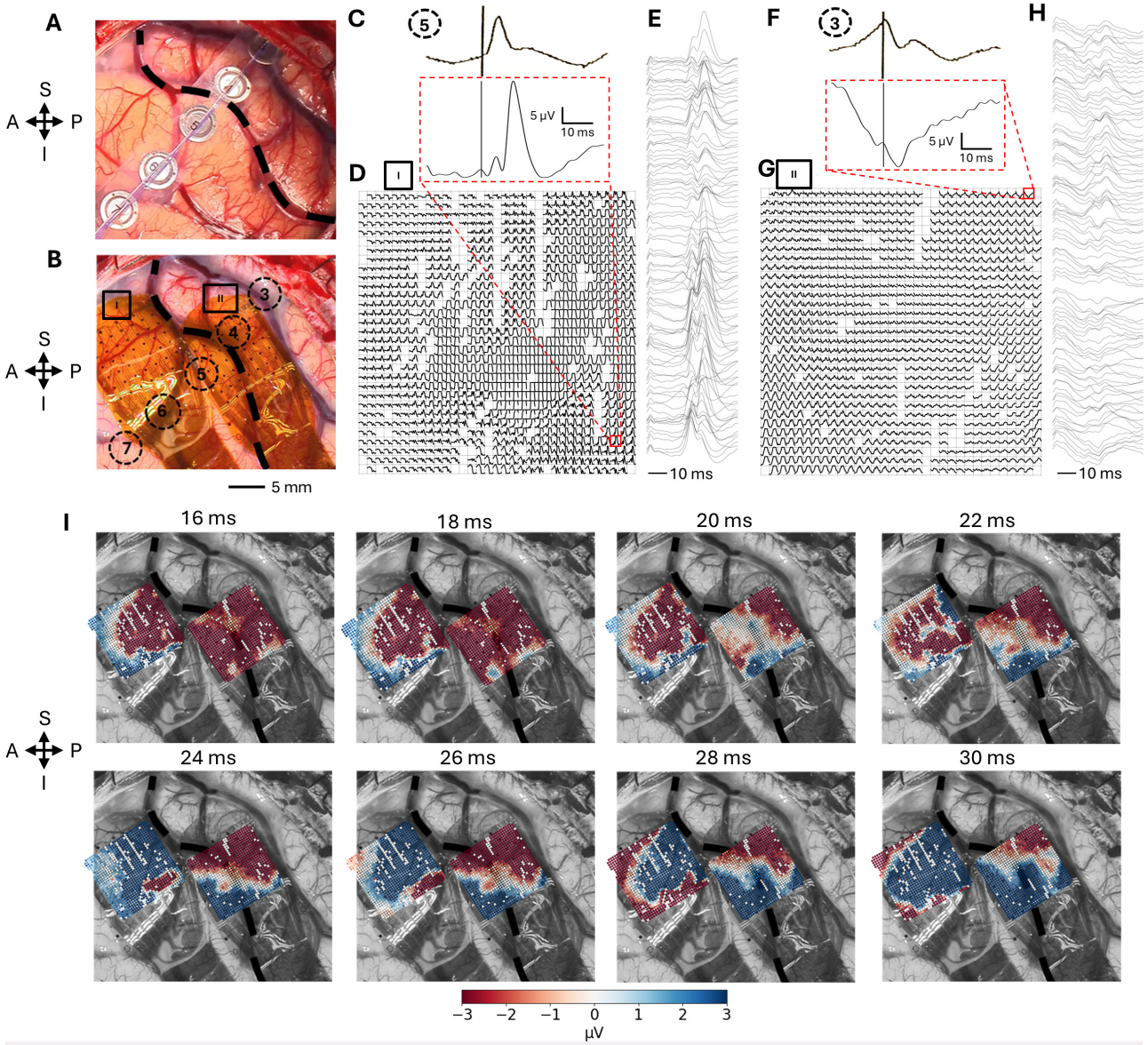

FIG. 4. Micro-ECoG arrays map the phase reversal of median nerve SSEPs across the central sulcus. *Dashed lines* indicate the estimated anatomical central sulcus in each image. Micro-μECoG SSEP waveforms were averaged across 75 stimulus trials and bandpass filtered at 10–300 Hz. The *arrows* indicate anatomical directions—anterior (A), posterior (P), superior (S), and inferior (I)—in each image. **A:** A macro-ECoG strip placed across the central sulcus (dashed line) during clinical intraoperative monitoring. **B:** Precision μECoG arrays placed across the central sulcus, with the prior position of the clinical macro-ECoG strip contacts indicated with *dashed circles*. Array I is over the postcentral gyrus, and array II is over the precentral gyrus. **C:** An SSEP from macro-ECoG contact 5 (*upper*) and an SSEP recorded by a microcontact (*lower*) positioned on the same area of the cortex as macro-ECoG contact 5. The *vertical line* indicates the 20-msec poststimulus time point. **D:** SSEPs recorded from each microcontact on μECoG array I. **E:** A total of 120 SSEPs were recorded by μECoG array I. **F:** An SSEP from macro-ECoG contact 3 (*upper*) and an SSEP recorded by a microcontact (*lower*) positioned on the same area of cortex as macro-ECoG contact 3. The *vertical line* indicates the 20-msec poststimulus time point. **G:** SSEPs recorded from each microcontact on μECoG array II. **H:** A total of 120 SSEPs were recorded by μECoG array II. **I:** Heatmaps of mean voltage from 75 stimulus trials recorded by the μECoG arrays through time. Each *dot* represents the mean voltage recorded by each microcontact at the poststimulus time point labeled above.

nonhuman primates mapping SSEPs with μECoG has shown propagation of SSEP activity from regions within the central sulcus to the postcentral gyrus.[9] Given the propagation of sensory information from within the central sulcus to the postcentral gyrus surface, inclusion of electrodes within the central sulcus may lead to more accurate and faster sensory decoding.[9] Matsuo et al.[10] previously described a neurosurgical protocol for central sulcus dissection in macaques, which reflects the general surgical technique used in this unique case requiring central sulcus dissection for tumor resection.[10] Such electrodes traversing the central sulcus in nonhuman primates have shown both higher somatosensory accuracy[9] and lower thresholds of activation for motor evoked potentials.[10] Notably, the availability of flexible μECoG arrays that can conform to the sulcus, such as the Precision array used in this case, is necessary for such intrasulcal recordings. The

Unauthenticated | Downloaded 02/21/26 07:00 PM UTC

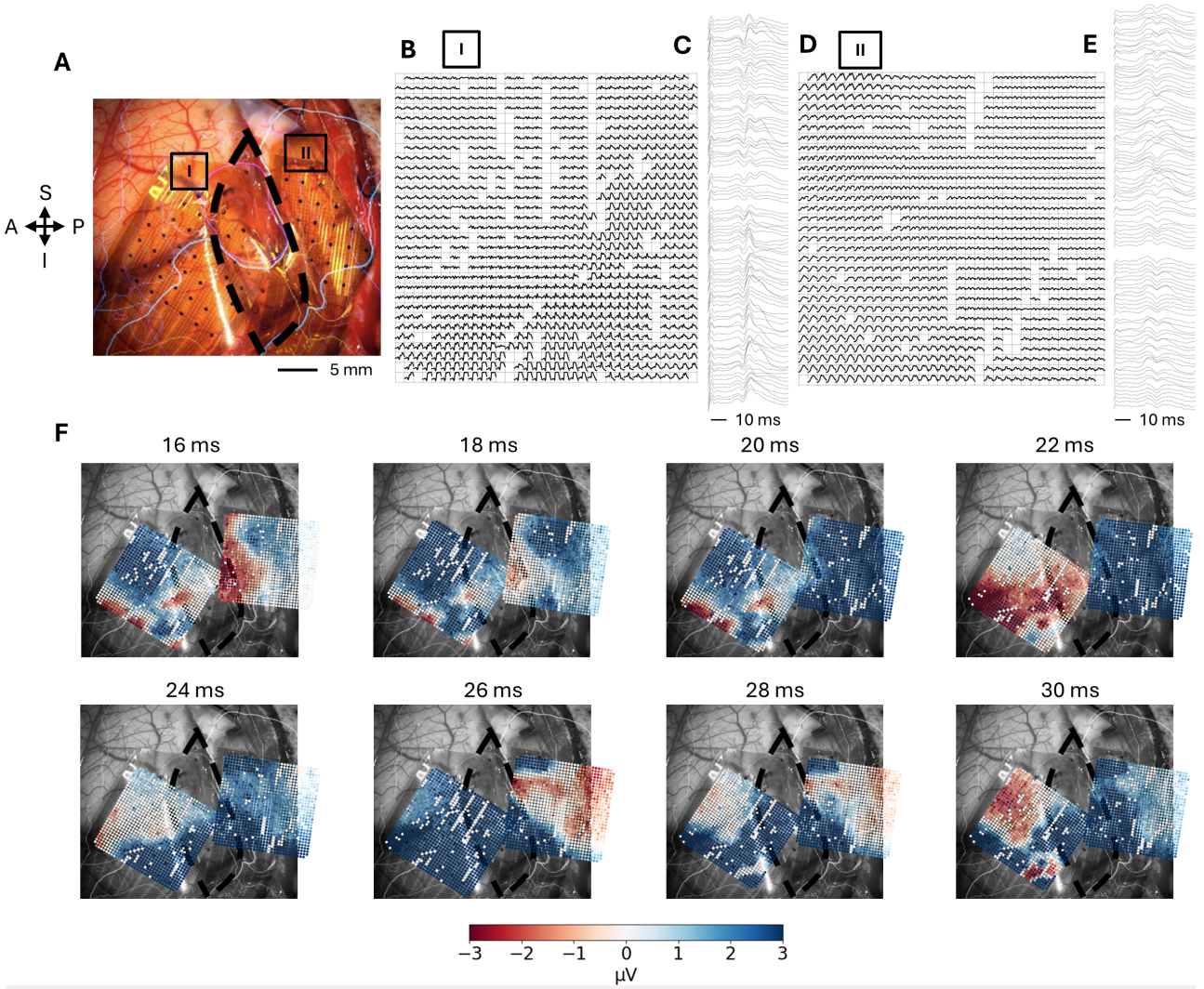

FIG. 5. Micro-ECoG arrays map the phase reversal of median nerve SSEPs across and within the opened central sulcus. *Dashed lines* indicate the estimated anatomical sulcus in each image. Micro-ECoG SSEP waveforms were averaged across 137 stimulus trials and bandpass filtered at 10–300 Hz. The *arrows* indicate anatomical directions: anterior (A), posterior (P), superior (S), and inferior (I). **A:** Precision μECoG arrays placed on the opened central sulcus, with edges of the array folded into the sulcus. Array I is over the postcentral gyrus and into the posterior central sulcus, and array II is over the precentral gyrus and into the anterior central sulcus. **B:** SSEPs recorded from each microcontact on μECoG array I. **C:** A total of 120 SSEPs were recorded by μECoG array I. **D:** SSEPs recorded from each microcontact on μECoG array II. **E:** A total of 120 SSEPs were recorded by μECoG array II. **F:** Heatmaps of mean voltage from 137 stimulus trials recorded by the μECoG arrays through time. Each *dot* represents the mean voltage recorded by each microcontact at the poststimulus time point labeled above.

mechanical flexibility of the μECoG arrays enables very close conformability of the high-density electrodes to the cortical surface without causing damage to the cortical tissue. Additionally, the amplification and digitization circuitry is very near to the recording sites (< 15 cm), reducing opportunities for coupling of environmental noise in the operating room. These design features enable high-fidelity recordings of cortical evoked potentials, comparable in signal quality to those captured by traditional Ad-Tech cortical strip electrodes (Fig. 3) but with much greater spatial resolution.

Limitations

As a preliminary report, the demonstrated findings require replication across further patients with varying neurosurgical interventions around the central sulcus. One limitation of the μECoG arrays is that they are limited to recording at the cortical surface. This precludes characterization of neuronal firing rates directly from pyramidal neurons at layers V and VI. Future work should investigate the relative contributions of each cortical layer to the summed local field potential captured by high-density surface microelectrodes by simultaneously recording from laminar depth electrodes and high-density ECoG arrays. Within the scope of the present work, we have not directly verified which layers contributed to the local field potential captured by our high-density ECoG array at the cortical surface. Signal-to-noise ratio was optimized in the operative environment through minimization of known potential electrical sources of noise in the operating room, and through prior experimentation to obtain optimal ground and reference

Unauthenticated | Downloaded 02/21/26 07:00 PM UTC

schemes (including a ground maintained on the forehead. However, the longer-term stability of signals recorded from the device was not explored and is an important area for further research.

We demonstrate the feasibility and utility of μECoG for sensorimotor mapping within the central sulcus, revealing a phase reversal at a resolution of approximately 400 microns. Compared to standard mapping, which records gyral surface electrophysiology, we further demonstrate phase-reversal electrophysiology within a dissected central sulcus. High-resolution cortical mapping from μECoG may foster several neurosurgical advancements, from tumor resection to brain-computer interfaces (BCIs). This case demonstrates the possibility of further temporospatial mapping with μECoG electrodes. However, further work is needed to assess the value of these electrodes for standard neurosurgical interventions across a larger number of patients, and for potential applications such as sensorimotor BCI.

Lessons

Mapping around the central sulcus is relevant to several neurosurgical conditions, many of which may benefit from high-density electrophysiological recordings. Standard ECoG strip arrays for tumor resection require several repeated SSEP measurements with varying array placements to identify the 2D morphology of the central sulcus.[11] Use of μECoG arrays can provide a clear mapping of the central sulcus in two spatial dimensions. Furthermore, as shown in Figs. 4 and 5, temporal evolution in the phase reversal can be assessed, which has been historically ignored with typical SSEP mapping. In addition to tumor resection, epileptic resections around the precentral gyrus require accurate delineation of the seizure onset zone while sparing functional regions of motor cortex. Such resections have relied on cortical grids with several millimeters of resolution between electrodes.[12] Micro-ECoG, as we exhibit in this case, may provide even higher-resolution discrimination between functional regions of cortex and abnormal regions safe for resection, such as epileptogenic lesions.

There may be significant interindividual variation in electrophysiological morphology of the central sulcus, which cannot be captured in granular detail using standard millimeter-resolution cortical arrays. For instance, using motor evoked potentials, cases of motor function within the postcentral gyrus have been identified.[13] Intraoperative knowledge of such individual variation is crucial for safe neurosurgical intervention and may be aided by high-density μECoG. Mapping using μECoG may limit the need for direct cortical stimulation for motor evoked potentials, thus facilitating more efficient mapping around the central sulcus and decreasing the likelihood of stimulation-induced seizures.[14] Central sulcus mapping with standard ECoG electrodes has long been established as a safe and effective tool for tumors around the central sulcus, with an efficacy of > 90%.[15] However, several neurosurgical indications may benefit from increased precision of functional mapping around the central sulcus with μECoG compared with standard ECoG arrays. These include mapping precise epileptic versus functional cortical regions around the central sulcus (where the target of ablation or neuromodulation is paramount) and increased ability to map the functional boundaries around high-grade gliomas (in which maximizing the extent of resection up to functional cortex is critical).

In addition to neurosurgical interventions for traditional indications such as epilepsy and tumor resection, high-resolution mapping of cortical electrophysiology between the precentral gyrus and postcentral gyrus may advance BCI technologies. To date, several successful applications of sensorimotor-based BCIs have been implemented. These applications have generally used electrical arrays with millimeter-level spatial resolution.[16–18] Higher spatial resolution provided by μECoG arrays may offer further accuracy and usability of sensorimotor BCIs. Prospective exploration of μECoG across the precentral and postcentral gyri, both intraoperatively during neurosurgical intervention and longitudinally for BCI applications, will help advance our understanding of human brain mapping.

Acknowledgments

We thank Jill Gregory, MFA, for her artistic contributions to this work.

References

1. Nii Y, Uematsu S, Lesser RP, Gordon B. Does the central sulcus divide motor and sensory functions? Cortical mapping of human hand areas as revealed by electrical stimulation through subdural grid electrodes. *Neurology*. 1996;46(2):360-367. doi:10.1212/WNL.46.2.360
2. Eichert N, Watkins KE, Mars RB, Petrides M. Morphological and functional variability in central and subcentral motor cortex of the human brain. *Brain Struct Funct*. 2021;226(1):263-279. doi:10.1007/s00429-020-02180-w
3. Kaiju T, Inoue M, Hirata M, Suzuki T. High-density mapping of primate digit representations with a 1152-channel μECoG array. *J Neural Eng*. 2021;18(3):036025. doi:10.1088/1741-2552/abe245
4. Wang X, Gkogkidis CA, Iljina O, et al. Mapping the fine structure of cortical activity with different micro-ECoG electrode array geometries. *J Neural Eng*. 2017;14(5):056004. doi:10.1088/1741-2552/aa785e
5. Salgado-Lopez L, Oemke H, Feng R, et al. Intraoperative use of heads-up display in skull base surgery. *Neurosurg Focus Video*. 2022;6(1):V2.
6. Asman P, Prabhu S, Bastos D, et al. Unsupervised machine learning can delineate central sulcus by using the spatiotemporal characteristic of somatosensory evoked potentials. *J Neural Eng*. 2021;18(4):046038. doi:10.1088/1741-2552/abf68a
7. Xie T, Wu Z, Schalk G, et al. Automated intraoperative central sulcus localization and somatotopic mapping using median nerve stimulation. *J Neural Eng*. 2022;19(4):046020. doi:10.1088/1741-2552/ac7dfd
8. Wang W, Degenhart AD, Collinger JL, et al. Human motor cortical activity recorded with Micro-ECoG electrodes, during individual finger movements. *Annu Int Conf IEEE Eng Med Biol Soc*. 2009;2009:586-589. doi:10.1109/IEMBS.2009.5333704
9. Kaiju T, Doi K, Yokota M, et al. High spatiotemporal resolution ECoG recording of somatosensory evoked potentials with flexible micro-electrode arrays. *Front Neural Circuits*. 2017;11:20. doi:10.3389/fncir.2017.00020
10. Matsuo T, Kawasaki K, Osada T, et al. Intrasulcal electrocorticography in macaque monkeys with minimally invasive neurosurgical protocols. *Front Syst Neurosci*. 2011;5:34. doi:10.3389/fnsys.2011.00034
11. Bharadwaj S, Venkatraghavan L. Intraoperative phase reversal monitoring using a novel technique. *J Neurosurg Anesthesiol*. 2016;28(1):82. doi:10.1097/ANA.0000000000000187
12. Simon MV, Cole AJ, Chang EC, et al. An intraoperative multimodal neurophysiologic approach to successful resection of precentral gyrus epileptogenic lesions. *Epilepsia*. 2012;53(4):e75-e79. doi:10.1111/j.1528-1167.2011.03400.x
13. Boerger TF, DeGroot AL, Schwartz S, Botros N, Schmit BD, Krucoff MO. Multimodal and repeated localization of primary hand motor function to the lateral postcentral gyrus in a case of frontal motor area brain metastasis. *Neurosurg Pract*. 2024;5(3):e24.00070. doi:10.1227/neuprac.0000000000000095
14. Simon MV, Sheth SA, Eckhardt CA, et al. Phase reversal technique decreases cortical stimulation time during motor

Unauthenticated | Downloaded 02/21/26 07:00 PM UTC

mapping. *J Clin Neurosci*. 2014;21(6):1011-1017. doi:10.1016/j.jocn.2013.12.015
15. Cedzich C, Taniguchi M, Schäfer S, Schramm J. Somatosensory evoked potential phase reversal and direct motor cortex stimulation during surgery in and around the central region. *Neurosurgery*. 1996;38(5):962-970. doi:10.1097/00006123-199605000-00023
16. Lorach H, Galvez A, Spagnolo V, et al. Walking naturally after spinal cord injury using a brain–spine interface. *Nature*. 2023;618(7963):126-133. doi:10.1038/s41586-023-06094-5
17. Cajigas I, Davis KC, Meschede-Krasa B, et al. Implantable brain–computer interface for neuroprosthetic-enabled volitional hand grasp restoration in spinal cord injury. *Brain Commun*. 2021;3(4):fcab248. doi:10.1093/braincomms/fcab248
18. Yadav AP, Li D, Nicolelis MAL. A brain to spine interface for transferring artificial sensory information. *Sci Rep*. 2020;10(1):900. doi:10.1038/s41598-020-57617-3

Disclosures

Dr. Barth reported paid salary and stock options from Precision Neuroscience and a patent pending for US20220370805A1. Dr. Ho reported personal fees from Precision Neuroscience during the conduct of the study, personal fees from Precision Neuroscience outside the submitted work, and pending patents for US20250114024A1 and US20240374207A1. Ms. Dister reported being a full-time employee of Precision Neuroscience and holding stock options in the company during the conduct of the study. Dr. Rapoport reported grant support and engineering study support to Mount Sinai related to this study, and personal fees and multiple patents issued as a cofounder and equity shareholder in Precision Neuroscience, which developed the electrode technology used in this study, and is a member of the Neurosurgery Department at Mount Sinai Hospital. Dr. Saez reported grants from Precision Neuroscience during the conduct of the study.

Author Contributions

Conception and design: Cummins, Ho, Fink Skular, Dister, Rapoport, Saez, Bederson. Acquisition of data: Cummins, Ho, Fink Skular, Dister, Rapoport, Saez, Bederson. Analysis and interpretation of data: Cummins, Barth, Ho, Fink Skular, Dister, Rapoport, Bederson. Drafting the article: Cummins, Barth, Rapoport, Bederson. Critically revising the article: Ho, Fink Skular, Rapoport, Saez, Bederson. Reviewed submitted version of manuscript: Cummins, Ho, Fink Skular, Dister, Rapoport, Bederson. Approved the final version of the manuscript on behalf of all authors: Cummins. Statistical analysis: Cummins. Administrative/technical/material support: Ho, Fink Skular, Dister, Bederson. Study supervision: Ho, Fink Skular, Dister, Bederson.

Supplemental Information

Videos

Video 1. https://vimeo.com/1145652842.

Correspondence

Daniel D. Cummins: Icahn School of Medicine at Mount Sinai, New York, NY. daniel.cummins@mountsinai.org.

Unauthenticated | Downloaded 02/21/26 07:00 PM UTC